Sensors and Actuators B 249 (2017) 506–514

Contents lists available at ScienceDirect

Sensors and Actuators B: Chemical

journal homepage: www.elsevier.com/locate/snb

Research Paper

Single-walled carbon nanotubes covalently functionalized with cysteine: A new alternative for the highly sensitive and selective Cd(II) quantification

Fabiana A. Gutierrez[a], Jose Miguel Gonzalez-Dominguez[b,1], Alejandro Ansón-Casaos[b], Javier Hernández-Ferrer[b], María D. Rubianes[a], María T. Martínez[b,*], Gustavo Rivas[a,*]

[a] INFIQC, Departamento de Físico Química, Facultad de Ciencias Químicas, Universidad Nacional de Córdoba, Ciudad Universitaria, 5000 Córdoba, Argentina
[b] Instituto de Carboquímica (CSIC), C/Miguel LuesmaCastán 4, E-50018 Zaragoza, Spain

ARTICLE INFO

Article history:
Received 11 January 2017
Received in revised form 28 March 2017
Accepted 6 April 2017
Available online 8 April 2017

Keywords:
Carbon nanotubes
Electrochemical sensor
Cadmium
Complex formation
Cysteine-functionalized SWCNT
Covalently functionalization

ABSTRACT

This work is focused on the development of an electrochemical sensor for the quantification of Cd(II) based on the use of glassy carbon electrodes (GCE) modified with a dispersion of single-walled carbon nanotubes (SWCNTs) covalently functionalized with cysteine (Cys). Cd(II) is preconcentrated at the electrode surface by complex formation at open circuit potential, followed by the reduction at −0.900 V and the final anodic voltammetric stripping in a 0.020 M acetate buffer solution pH 5.00. The functionalization of SWCNTs was performed through the reaction between the carboxylic groups of oxidized SWCNT and amino groups of S-triphenylmethyl cysteine using a coupling chemistry agent based on benzotriazol for the activation of carboxylic residues.

There was a linear relationship between Cd oxidation signal and Cd(II) concentration between 1.0 and 300.0 μgL^{-1} Cd(II), with a sensitivity of $(49 \pm 2) \times 10^{-3}$ $\mu A \mu g^{-1} L$ and a detection limit of 0.3 μgL^{-1}. The reproducibility was 1.7% using the same dispersion and 3.8% using 3 different dispersions. The sensor was challenged with groundwater samples enriched with Cd(II) showing excellent recovery percentages and excellent agreement with the values obtained by ICP-MS.

1. Introduction

The control of the amount of heavy metals released to the environment has received enormous attention in the last years due to the direct impact on the human health and the economic damage associated with the contamination problems [1,2]. Several methodologies have been proposed for the detection of heavy metals, including atomic absorption spectrometry (AAS), inductively coupled plasma optical emission spectrometry (ICP-OES), inductively coupled plasma mass spectrometry (ICP-MS), neutron activation analysis (NAA), X-ray fluorescence (XRF), and ion chromatography (IC) [3–9]. However, although these techniques offer high sensitivity and selectivity, they present some disadvantages that restrict their routine use like complex sample preparation, use of sophisticated instruments, and the requirement of skilled personnel. Electrochemical techniques have demonstrated to be an important alternative due to their simplicity, relatively low cost, sensitivity, possibility of miniaturization and descentralized work [10].

Different electrochemical sensors have been proposed. Ghaemi et al. [11] have reported a ion-selective sensor for Cd quantification based on the use of 1,13-bis (8-quinolyl)-1,4,7,10,13-pentaoxatridecane as supramolecular carrier. p-*tert*-butylcalix[6]arene has been demonstrated to be a very efficient membrane for the development of fast, reproducible, stable and selective Cd ion-selective electrodes [12]. Chow et al. [13] have proposed the nanomolar detection of Cu(II), Cd(II) and Pb(II) mixtures at gold electrodes modified with thioctic acid and peptides. Yantasee et al. [14] have detected Cu(II), Cd(II) and Pb(II) in non-pretreated natural waters using glassy carbon electrodes (GCE) modified with thiol functionalized mesoporous silica and Nafion Bismuth film electrode, introduced in 2000 by Wang et al. [15] have demonstrated to be highly successful for the quantification of heavy metal ions at sub μgL^{-1} level [16–19].

* Corresponding authors.
E-mail addresses: mtmartinez@icb.csic.es (M.T. Martínez), grivas@fcq.unc.edu.ar, rivasgus@yahoo.com.ar (G. Rivas).
[1] Current address: MSOC-Nanochemistry Group, Faculty of Chemistry, Universidad de Castilla-La Mancha, Avda, Camilo José Cela S/N, 13071, Ciudad Real, Spain.

http://dx.doi.org/10.1016/j.snb.2017.04.026
0925-4005/

Antimony film [20,21] and stannum film [22,23] electrodes have been also used for the sensitive quantification of Cd(II).

Nanomaterials have demonstrated to be very useful for the development of electrochemical sensors due to their unique mechanical, magnetic, electrical, optical, and catalytic properties [24–27]. Wu et al. [28] have described the electrochemical determination of Hg(II), Cu(II), Pb(II) and Cd(II) using GCE modified with mesoporous MgO nanosheets. A sensitive detection of Tl(I), Pb(II) and Hg(II) has been proposed using anionic liquid/graphene/carbon paste electrode [29]. Ruecha et al. [30] have described an electrochemical sensor for the simultaneous detection of Zn(II), Cd(II) and Pb(II) using a graphene–polyaniline nanocomposite electrode. The incorporation of graphene oxide at 4-aminophenyl modified gold electrodes have demonstrated to be highly successful for the sensitive quantification of Pb(II), Cd(II) and Hg(II) [31]. Carbon nanotubes modified with different ligands have been also used for the quantification of heavy metals [32–35].

The motivation of this work was to transfer the fascinating ability of Cys to complexate heavy metals [36–38] to the development of an electrochemical sensor for the quantification of Cd (II) based on the modification of GCE with a dispersion of single-walled carbon nanotubes (SWCNT) covalently functionalized with L-cysteine (Cys) (SWCNT-Cys) and the efficient complex formation between HS residues of Cys and Cd(II) [37,38].

It is widely known that carbon nanotubes (CNTs) need to be functionalized to facilitate the dispersion in aqueous media and to make possible the preparation of CNT-based electrochemical sensors [39–42]. We have recently reported an electrochemical sensor for Cu(II) based on the use of GCE modified with multi-walled carbon nanotubes non-covalently functionalized with polyhistidine (GCE/MWCNT-Polyhistidine) through the complex formation of Cu(II) with the histidine residues present at GCE/MWCNT-Polyhistidine [39]. Morton et al. [43] have proposed the modification of GCE with oxidized multi-walled carbon nanotubes (MWCNT) covalently functionalized with cysteine (Cys), although in this case they have used the carbodiimide/N-hydroxysuccinimide chemistry, a strategy completely different to the one we are proposing here and without using protective groups for thiol groups. The resulting sensor has been used for the quantification of Cu(II) and Pb(II), although the analytical performance was not really competitive compared to previously reported electrochemical sensing strategies. A similar modification scheme has been also used as a sorbent for preconcentration of heavy metals [39].

In the following sections we report the synthesis of the Cys-modified SWCNT; the characterization of the resulting modified nanostructures using different techniques (FTIR, Raman, TGA, XPS, and electrochemical techniques); and the analytical application of GCE/SWCNT-Cys for the highly sensitive and selective quantification of Cd(II).

2. Experimental

2.1. Materials and reagents

Single walled carbon nanotubes (SWCNT, AP-SWNT grade) were purchased from Carbon Solutions Inc. (Riverside, California). Sodium dodecylbenzenesulfonate (SDBS), anhydrous *N*,*N*'-dimethylformamide (DMF), O-(benzotriazol-1-yl)-*N*,*N*,*N*′,*N*′-tetramethyluronium hexafluorophosphate (HBTU), *N*,*N*-diisopropylethylamine (EDIPA), S-triphenylmethylcysteine(S-Trt-Cys), trifluoroacetic acid (TFA), triethylsilane (Et_3Si), dichloromethane, diethyl ether, quinone (Q) and hydroquinone (H_2Q) were purchased from Sigma-Aldrich. Hydrogen peroxide (30% v/v aqueous solution), $Hg_2(NO_3)_2{\cdot}H_2O$, $(CdSO_4)_3.8H_2O$ and $Pb(CH_3COO)_2Pb(OH)_2$ were received from Anedra. Other chemicals were reagent grade and used without further purification.

A 0.200 M acetate buffer solution pH 5.00 was used as supporting electrolyte. Ultrapure water ($\rho = 18\ M\Omega\ cm^{-1}$) from a Millipore-MilliQ system was used for preparing all the solutions. All the experiments were conducted at room temperature.

2.2. Apparatus

Electrochemical experiments were performed with Epsilon (BAS), TEQ 4 and Autolab PGSTAT128 N potentiostats. The electrodes were inserted into the cell (BAS, Model MF-1084) through holes in its Teflon cover. A platinum wire and Ag/AgCl, 3 M NaCl (BAS, Model RE-5B) were used as counter and reference electrodes, respectively. All potentials are referred to the latter. A magnetic stirrer (BASi Cell stand) set at 800 rpm and a stirring bar provided the convective transport during the amperometric measurements.

Infrared spectroscopy (FTIR) measurements were performed with a Bruker Vertex 70 spectrometer. The samples were prepared with spectroscopic-grade KBr. Micro Raman spectroscopy experiments were performed with a HORIBA JobinYvon spectrometer (model HR 800 UV) using a green laser at 532 nm.

X-ray photoelectron spectroscopy (XPS), was performed with an ESCAPlus Omicron spectrometer equipped with a Mg anode (1253.6 eV) working at 150 W (15 mA, 10 kV). CASA software was used for the peak deconvolution.

Thermogravimetric analysis (TGA) were carried out with a Setaram balance, model Setsys Evolution 16/18. The experiments were performed using a nitrogen inert flow and a heating ramp of $10\ ^{\circ}C min^{-1}$.

Sonication treatments were carried out with a sonicator probe VCX 130W (Sonics and Materials, Inc.) of 20 kHz frequency with a titanium alloy microtip (3 mm diameter).

Amperometric experiments were performed in an acetate buffer solution (0.020 M, pH 5.00) by applying the desired potential and allowing the transient current to decay to a steady-state value prior to the addition of the analyte and subsequent current monitoring.

Electrochemical impedance spectroscopy (EIS) experiments were carried out in a 0.020 M acetate buffer solution pH 5.00 by applying a sinusoidal potential perturbation of 10 mV in the frequency range of 10^5–10^{-1} Hz and a working potential corresponding to the formal potential of a 2.0×10^{-3} M Q/H_2Q solution (0.050 V). The impedance spectra were analyzed and fitted using the Z-view program.

2.3. Synthesis of functionalized SWCNT

From the scarce reports found for the covalent functionalization of CNTs with Cys [39,43] the use of the bare aminoacid is a common feature. With this approach, it is difficult to ascertain if the reaction occured through classical amidation or thioester formation (which may also be formed with carbodiimides) [44]. In this work, we have undertaken the functionalization using thiol-protected Cys to avoid thioester formation, and we have set the reaction conditions to guide the amide bond formation throughout the α-amino group of Cys and to hinder any unwanted side-reaction such as peptidic condensation.

SWCNT were purified by oxidation at 350 °C for 2 h under air atmosphere and further reflux in 3 M HCl for 2 h. Purified SWCNT were oxidized in a 3 M H_2SO_4/HNO_3 mixture (50:50 v/v) by refluxing for 3 h (called SWCNT-Ox) Once filtered, rinsed with deionized water and over-dried, the solid was functionalized with Cys (SWCNT-Cys). In a typical experiment, 100 mg of SWCNT-Ox were placed in a round-bottom flask and bath-sonicated for 1 h in a 0.5% w/v sodium dodecyl benzene sulfonate (SDBS) aqueous solution. After that, the suspension was transferred to a Schlenk

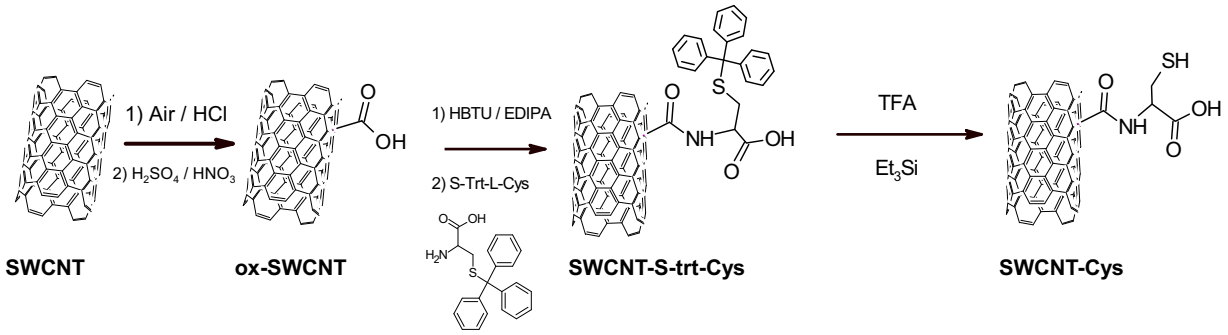

Scheme 1. Reaction pathways for the functionalization of SWCNTs with S-trt-Cys.

flask, purged with Ar under magnetic stirring, and cooled with a water/ice bath. The COOH residues of SWCNT-Ox were activated with 300 mg of HBTU and 1 mL of EDIPA while the medium was kept at 0 °C for 45 min. Once activated, a volume of 100 mL of 8.1 mM S-trt-Cys solution (prepared in DMF) was dropwise incorporated to the SWCNT dispersion in a period of 24 h, at room temperature. The reaction was allowed to take place at room temperature for 48 h and under these conditions, the covalent attachment of Cys was intended through the α-amine of L-Cys. A gentle continuous flow of Ar and magnetic stirring were kept along the whole functionalization process. The reaction product was filtered through a 0.1 μm pore size Teflon membrane and washed with DMF, ethanol and acetone (Scheme 1).

The deprotection of the aminoacid was performed by cleaving the tritylprotective groups with TFA [45] and Et_3Si acting as a scavenger [46]. An amount of 100 mg of SWCNT-S-Trt-Cys powder was redispersed in 25 mL of dichloromethane by sonication with an ultrasounds bath. After the addition of 1 mL of TFA and 5 eq. of Et_3Si, the mixture was left at room temperature for 2 h under stirring conditions and finally filtered through a 0.1 μm pore size Teflon membrane, rinsed with dichloromethane and diethyl ether, and dried under vacuum at room temperature (Scheme 1).

2.4. Preparation of GCE modified with SWCNT-Cys

2.4.1. Preparation of SWCNT-Cys dispersion

The dispersion was obtained by sonicating 0.5 mg of SWCNT-Cys with 1.0 mL of water for 5.0 min with ultrasonic probe. Dispersions of SWCNT and SWCNT-Ox were prepared in a similar way.

2.4.2. Modification of GCE with SWCNT-Cys (GCE/SWCNT-Cys)

GCEs were polished with alumina slurries of 1.0, 0.30, and 0.05 μm for 2 min each. Before modification with SWCNT-Cys, the electrodes were cycled (10 cycles) in a 0.050 M phosphate buffer solution pH 7.40 between −0.300 V and 0.800 V at 0.050 Vs^{-1}. The modification was performed by immobilization of an aliquot of 20 μL of SWCNT-Cys dispersion on top of the GCE and the solvent was allowed to evaporate at room temperature. The modified electrodes were cycled for ten times between −0.200 V and 0.800 V at 0.050 V/s before starting the electrochemical experiments. GCE/SWCNT and GCE/SWCNT-Ox were prepared in a similar way by using the corresponding dispersions.

2.5. Quantification of Cd(II)

The steps for the quantification of Cd(II) are the following:

2.5.1. Preconcentration

Performed at open circuit potential by immersion of GCE/SWCNT-Cys in the Cd(II) solution (prepared in a 0.020 M acetate buffer pH 5.00) for 5.0 min under stirring conditions.

2.5.2. Washing

The GCE/SWCNT-Cys containing the preconcentrated Cd(II) was washed with a 0.020 M acetate buffer solution pH 5.00 for 10 s and then transferred to a fresh acetate buffer solution.

2.5.3. Reduction

The preconcentrated Cd(II) was reduced at −0.900 V for 180 s in a 0.020 M acetate buffer solution pH 5.00.

2.5.4. Stripping

The anodic stripping was performed in a 0.020 M acetate buffer solution pH 5.00 by scanning the potential between −0.900 V and 0.500 V at 0.010 V/s using Linear sweep voltammetry staircase (Step potential: 0.032 V).

The analytical signals were obtained from the oxidation currents of the accumulated and further reduced Cd(II) after substracting the background currents. All measurements were performed at room temperature.

3. Results and discussion

3.1. Characterization of SWCNT-Cys

3.1.1. FTIR spectroscopy

Fig. 1A displays the FTIR spectra for SWCNT-Ox and SWCNT-Cys. FTIR spectrum for SWCNT-Ox show bands associated to the presence of oxygenated groups, typically at 1100 cm^{-1} (C—O stretching), 1320 cm^{-1} (OH stretching), and 1727 cm^{-1} (C=O stretching). The presence of the carboxylate ion can be also detected from the bands at 1580–1620 cm^{-1} and 1320 cm^{-1} [47,48]. After functionalization with Cys, the consumption of COOH groups is denoted by the change in the ratio between the intensity of the band at 1723 cm^{-1} and the intensity of the rest of carboxylic-based bands. This region becomes more populated after reaction, exhibiting the most important contribution between 1600 and 1624 cm^{-1}, which corresponds to the amide bond. The functionalization with Cys also causes a pronounced increase in the intensity of Csp^3-H vibrations in methylene groups (~2840–2950 cm^{-1}), associated to the aliphatic segments of the functional groups. The bands due to the stretching of S–H and C–S (2550–2600 cm^{-1}) were not observed in the spectrum of SWCNT-Cys possibly due to the strong interactions between Cys and SWCNT and the small amount of Cys attached to the CNT [49].

It is interesting to note that two new IR bands appear after functionalization with Cys, that may be ascribed to the carboxylic

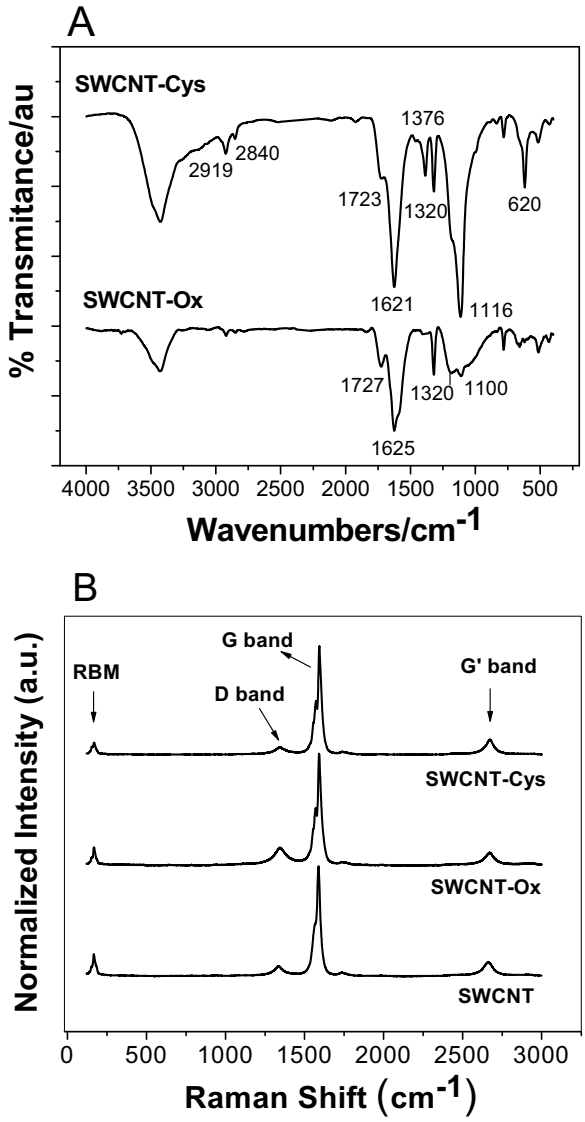

Fig. 1. A) FT-IR spectra for: SWCNT-Ox and SWCNT-Cys. B) Raman spectra for: SWCNT, SWCNT-Ox and SWCNT-Cys.

acid group present in the aminoacid moiety [50]. One is located at 620 cm^{-1} and could be attributed to the stretching vibration of the HC—COOH bond, while the other band at 1376 cm^{-1} is characteristic of the symmetric stretching of α-aminoacid's CO2 [50]. We may also discern the existence of amide N—H bands, whose stretching vibrations typically appear in the range of 1390–1430 cm^{-1} with a narrow weak-intensity fashion [45], and whose bending (1610–1630 cm^{-1}) and rocking (1100–1110 cm^{-1}) vibrations in Cys [50] could explain the sharpening of these two regions in our IR spectrum.

3.1.2. Raman spectroscopy

Fig. 1B shows typical Raman spectra for SWCNT, SWCNT-Ox and SWCNT-Cys. All the spectra present the radial breathing mode (RBM) at low frequencies, the D band at around 1300–1400 cm^{-1}, and the tangential multifeature G-band at around 1600 cm^{-1}. G-band presents the doublet structure (split into G+ and G− components) characteristic of semiconducting/metallic SWCNT [51]. The comparison of SWCNT and SWCNT-Ox spectra (Fig. 1B and Table 1) shows an increment in the D/G ratio and a shifting of the G and D bands to higher wavenumbers, associated to the presence of defects

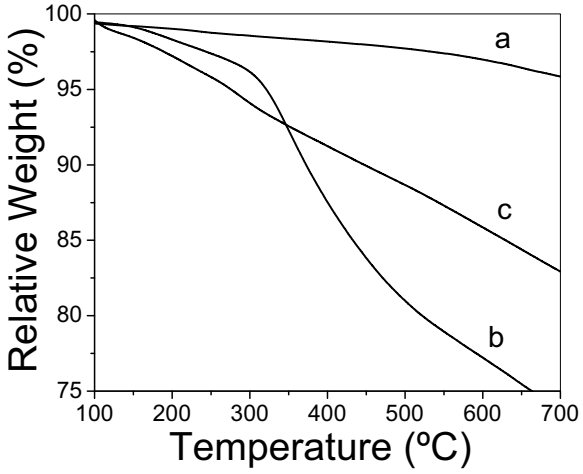

Fig. 2. TGA plots for: (a) SWCNT, (b) SWCNT-Ox, (c) SWCNT-Cys.

and disorder in the graphitic material due to the conversion of sp^2 carbons into sp^3 by the action of the strong oxidative treatment [52,53]. The changes of full widths at half maximum (FWHM) for D and G bands are associated to the presence of basal plane defects due to the vacancies and oxygenated groups at the graphitic structure [54]. After functionalization with Cys, the wavenumbers of D and G bands are higher than those for SWCNT and slightly smaller than those for SWCNT-Ox, while the D/G ratio decreases due to the partial deoxygenation and restoration of the sp^2 conjugated network after TFA treatment and the steric stress due to the newly formed amide bonds on the surface of SWCNT-Ox [54].

3.1.3. TGA

Fig. 2 shows TGA profiles obtained for SWCNT (a), SWCNT-Ox (b) and SWCNT-Cys (c). The slight weight loss (∼6 wt%) observed in the thermograms corresponding to SWCNT (Fig. 2a) indicates that they possess a very low amount of functional groups and that the oxygenated residues incorporated upon air oxidation are mostly removed during the HCl reflux. In the case of SWCNT-Ox (Fig. 2b), the amount of carboxylic groups, estimated from the release observed between 150 and 300 °C, was 0.66 mmol/g SWCNT. The weight loss observed between 300 and 500 °C is associated with the desorption of other oxygenated groups, mostly quinones, phenols and acid anhydrides [55,56].

In the case of SWCNT-Cys sample, considering the temperature frame of 150–350 °C (beyond which a simple α-aminoacid with no aromatic residues should be already pyrolyzed), the absolute difference in weight loss between SWCNT-ox and SWCNT-Cys may be ascribed to the amount of anchored Cys. The progressive mass loss beyond 350 °C is less steep in SWCNTs-Cys than in SWCNTs-ox, indicating the higher thermal stability of functionalized SWCNTs, in good agreement with the fact that the oxidized sample experienced a deoxygenation during the last step of the functionalization process (TFA treatment). These results give an additional support to the lower D-band observed in Raman spectroscopy.

3.1.4. XPS

Fig. 3 shows the C1s (Fig. 3A) and N1s (Fig. 3B) core level spectra of SWCNT-Cys, which include several components ascribed to the different covalent bonds present in the sample. All the deconvoluted bands match those reported for Cys [57]. The functionalization of SWCNTs-ox with Cys provides C—H, C—N and C—S bonds which are gathered in the band at 285.1 eV, representing a 25.8% of the total area in this region. Subsequent bands at 286.3 (C—O bonds), 287.5 (C=O bonds) and 288.8 eV (O—C=O bonds) could correspond to the remaining oxygen groups on the surface of

Table 1
RAMAN parameters obtained from data at Fig. 1B.

	Peak position of D band/cm^{-1}	Peak position of G band/cm^{-1}	D FWHM/cm^{-1}	G FWHM/cm^{-1}	D/G relation
SWCNT	1335	1588	64	25	0.09 ± 0.01
SWCNT-ox	1345	1594	92	26	0.15 ± 0.03
SWCNT-Cys	1344	1592	77	24	0.069 ± 0.005

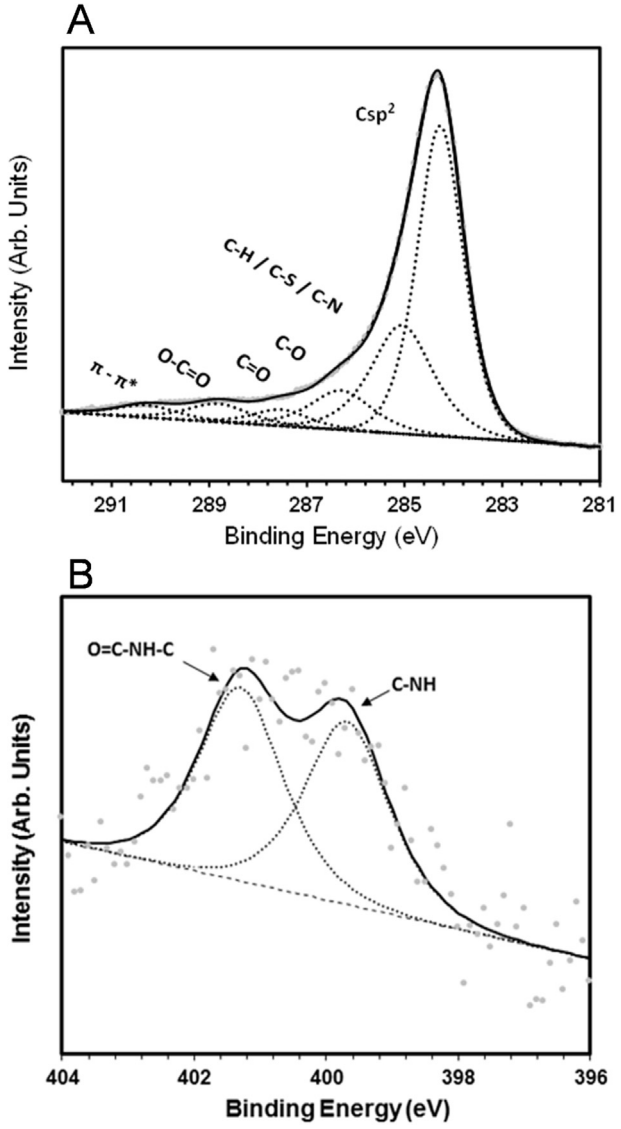

Fig. 3. Deconvoluted (A) C1s and (B) N1s XPS spectra of SWCNT-Cys.

SWCNTs, such as phenols, lactones or non-reacted carboxylic acids. The band at 290.3 eV is often observed for carbon nanotubes and is assigned to the π-π* transitions in delocalized structures containing sp^2 carbon bonds [58]. The N1 s spectrum (Fig. 3B) presents two main components, with nearly the same area ratio, namely the band corresponding to C—NH bond at 399.7 eV and the one corresponding to O=C—NH—C bonds at 401.3 eV [59]. Both are present in amide linkages but only the latter one is exclusive to them.

3.1.5. Electrochemical impedance spectroscopy and amperometry

The electronic properties of GCE/SWCNT-Cys were characterized by EIS. Fig. 4 depicts the Nyquist plots obtained for GCE/SWCNT (a), GCE/SWCNT-Ox (b) and GCE/SWCNT-Cys (c) at 0.050 V using 2.0×10^{-3} M Q/H$_2$Q solution as redox marker. The experimental data were fitted with a Randles circuit (where R$_s$ is the electrolytic

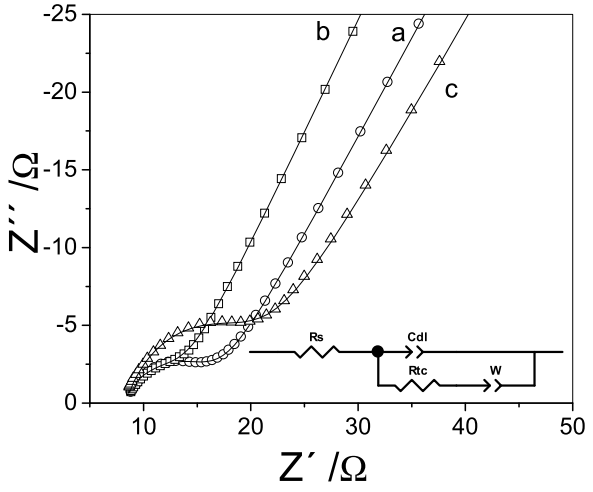

Fig. 4. Niquist plots for the impedance spectra obtained for different electrodes: GCE/SWCNT (a), GCE/SWCNT-Ox (b) and GCE/SWCNT-Cys (c). Frequency range: 10 KHz to 10 mHz; Potential perturbation: 10 mV; Working potential: 0.050 V. Redox indicator: 2.0×10^{-3} M Q/H$_2$Q solution. Supporting electrolyte: 0.020 M acetate buffer solution pH 5.00.

resistance, R$_{ct}$ the charge transfer resistance, C$_{dl}$ the double layer capacitance and W the Warburg impedance). R$_{ct}$ decreases when GCE is modified with SWCNT-Ox ((8.4 ± 0.4) vs (6.7 ± 0.5) Ω for GCE/SWCNT and GCE/SWCNT-Ox, respectively), indicating that the presence of the oxygenated groups facilitates the charge transfer for the couple Q/H$_2$Q. In the case of GCE/SWCNT-Cys (c) the R$_{ct}$ is almost the double than the one obtained for GCE/SWCNT-Ox ((11.9 ± 0.2) vs (6.7 ± 0.5) Ω), suggesting that Cys residues partially block the surface of SWCNT, hindering the charge transfer of the redox probe.

In order to obtain additional information about the accessibility of CNTs for the charge transfer and to make a correlation with the EIS results, we also performed amperometric determinations at 0.700 V at GCE/SWCNT-Ox and GCE/SWCNT-Cys using hydrogen peroxide as redox indicator. The sensitivity obtained at GCE/SWCNT-Ox ((13.5 ± 0.2) μAmM^{-1}) was almost 2.6 times higher than the one obtained at GCE/SWCNT-Cys ((5.5 ± 0.3) μAmM^{-1}), confirming that the functionalization of SWCNT-Ox with Cys produces a partial blockage of the charge transfer. These results represent an additional evidence, in an indirect way, of the efficient functionalization of SWCNT-Ox with Cys.

3.2. Analytical applications of GCE/SWCNT-Cys for the quantification of Cd(II)

As it was previously indicated, Cd(II) is accumulated at GCE/SWCNT-Cys at open circuit potential through the complex formation with the SH residues of Cys [38,45], it is further reduced at −0.900 V and finally reoxidized by scanning the potential from −0.900 V to 0.500 V. The optimization of the different conditions was performed through the evaluation of Cd(II) oxidation signal.The effect of the amount of SWCNT on the oxidation current of Cd was evaluated using GCE modified with dispersions containing different amount of SWCNT-Cys from 0.25 to 2.00 mgmL^{-1} (Fig. SI-1A). Cd-oxidation currents increase almost linearly with the

amount of SWCNT-Cys up to 0.50 mgmL^{-1}, to remain almost constant thereafter due to a saturation effect. Therefore, the selected amount of SWCNT-Cys was 0.50 mgmL^{-1}.

Considering that the analytical signal of the sensor is obtained from the oxidation of Cd present at GCE/SWCNT-Cys, the selection of the conditions for Cd(II) accumulation and Cd(II) reduction is critical to ensure an efficient analytical performance. Fig. SI–1B displays the effect of the accumulation time of Cd(II) at GCE/SWCNT-Cys at open circuit potential on the oxidation signal of Cd (from 1.0 to 10.0 min). The peak current increases with the preconcentration time from 1.0 to 5.0 min, to remain almost constant thereafter due to the saturation of the available complexing sites. Hence, a preconcentration time of 5.0 min was selected for further work. The effect of the potential applied to reduce the preconcentrated Cd(II) was evaluated between −1.200 V and −0.800 V. The best compromise between sensitivity, reproducibility and resolution of the final oxidation signal of Cd was obtained by applying a potential of −0.900 V. More negative potentials are not convenient due to the generation of hydrogen bubbles that makes the signal highly irreproducible. The oxidation current of Cd increases with the time that the electrode is hold at −0.900 V up to 180 s, to keep almost constant for longer times. Thus, the reduction of the accumulated Cd(II) was performed by applying −0.900 V for 180 s.

Before presenting the analytical performance of GCE/SWCNT-Cys, is important to discuss the advantages of the covalent attachment of Cys to SWCNT-Ox on Cd(II) sensing. We evaluate these advantages by comparing the response obtained for 300.0 μgL^{-1} Cd(II) at GCE/SWCNT, GCE/SWCNT-Ox and GCE/SWCNT-Cys (Fig. 2-SI). No voltammetric signal was obtained at GCE/SWCNT since no Cd was accumulated, while at SWCNT-Ox the oxidation signal for the preconcentrated and further reduced Cd(II) was 20 times lower than the one obtained at GCE/SWCNT-Cys ((0.24 ± 0.03) vs (4.9 ± 0.7) μA at SWCNT-Ox and GCE/SWCNT-Cys, respectively). No peaks were obtained at GCE/SWCNT-Cys in the absence of Cd(II). These results clearly demonstrate that, even when the carboxylate residues of SWCNTox allow the accumulation of Cd(II) by complex formation and facilitated electrostatic interaction, there is a selective preconcentration of Cd(II) at GCE/SWCNT-Cys due to the complex formation with Cys residues.

Fig. 5A shows the voltammetric response obtained after preconcentration of increasing concentrations of Cd(II) at GCE/SWCNT-Cys for 5.0 min at open circuit potential, followed by a reduction step at −0.900 V for 180 s and the final anodic voltammetric stripping in a 0.020 M acetate buffer solution pH 5.00. A well-defined response is observed in the whole range of concentrations from 1.0 to 300.0 μgL^{-1} Cd(II). A small shifting in the oxidation peak potential towards positive values is observed with the increment of Cd(II) concentration. The corresponding calibration plot is shown in Fig. 5B. A linear relationship between the oxidation signal and Cd(II) concentration is obtained between 1.0 and 300.0 μgL^{-1} with a sensitivity of (49 ± 2) x 10^{-3} μAμg^{-1}L and a detection limit of 0.3 μgL^{-1} (calculated as 3 x σ/S, where σ is the standard deviation of the blank signal and S the sensitivity). The reproducibility, obtained from the sensitivity of different calibration plots, was 1.7% using the same SWCNT-Cys dispersion and 4 different electrodes, and 3.8% using 3 different dispersions and 4 electrodes per dispersion.

The selectivity of the assay was evaluated by challenging the sensor with different metals. Fig. 5C shows the voltammetric response for 20 μgL^{-1} Cd(II) in the absence and presence of 100 μgL^{-1} Pb(II), Hg(II), Co(II), Zn(II), Ni(II), Cr(III), As(III), Ir (IV) and 20 μgL^{-1} Cu(II). Four well-defined oxidation current peaks were obtained at −0.760, −0.580,−0.093, and 0.28 V for Cd(II), Pb(II), Cu(II) and Hg(II), respectively. The Cd oxidation peak currents obtained in the absence (0.799 ± 0.08) μA and presence (0.789 ± 0.09) μA of Pb(II), Hg(II), Co(II), Zn(II), Ni(II), Cr(III), As(III),

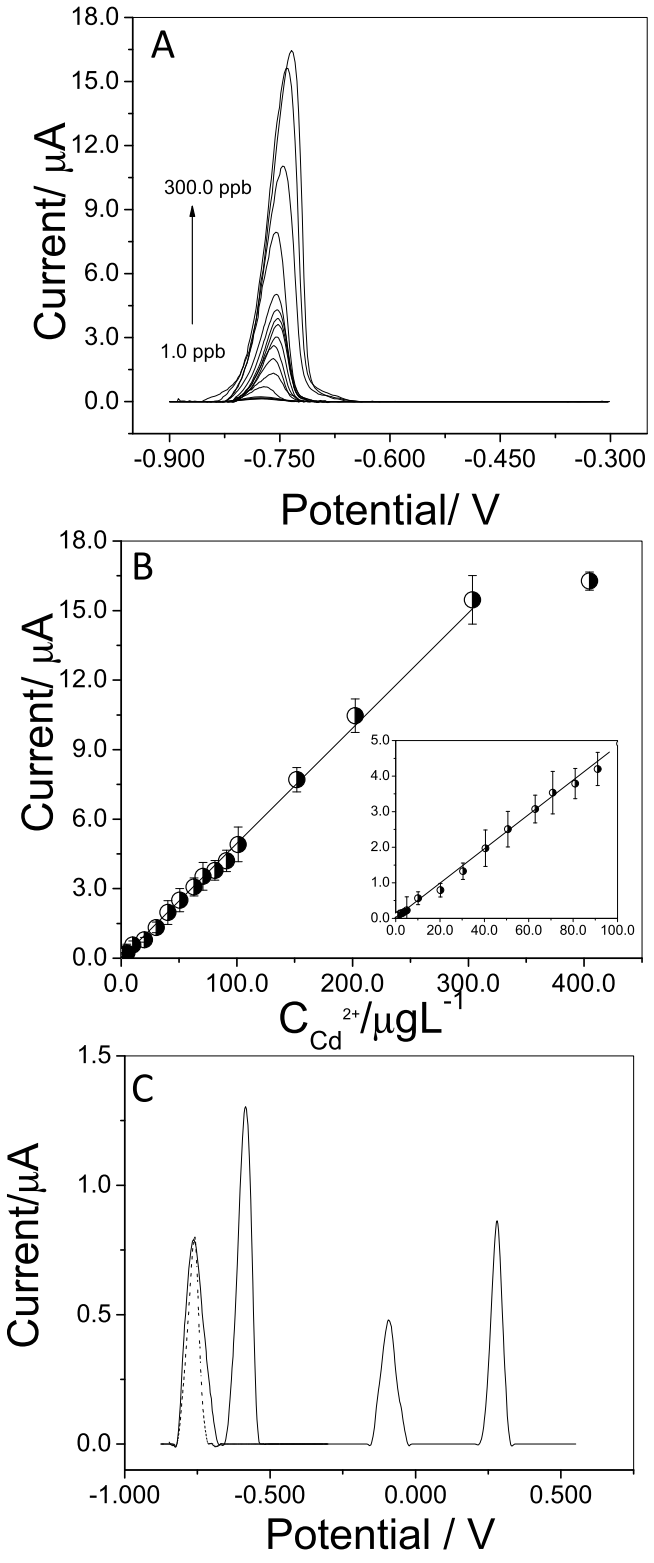

Fig. 5. (A)Voltammetric response obtained after preconcentration of different concentration of Cd(II) (from 1.0 μgL^{-1} and 300.0 μgL^{-1}) at GCE/SWCNT-Cys at open circuit potential for 5.0 min, followed by a reduction step at −0.900 V for 180 s and the final anodic voltammetric stripping in a fresh 0.020 M acetate buffer solution pH 5.00. (B) Calibration plot for Cd(II) obtained from the peak currents corresponding to the LSV recordings. (C) Linear scan voltammograms for 20 μgL^{-1} Cd(II) in the absence (dashed line) and presence (solid line) of 100 μgL^{-1} Pb(II), Hg(II), Co(II), Zn(II), Ni(II), Cr(III), As(III), Ir (IV) and 20 μgL^{-1} Cu(II).

Table 2
Comparison of the analytical performance of GCE/SWCNT-Cys with those of different methods reported for the detection of Cd(II).

Electrode	Electrochemical stripping technique	Procedure	Sensitivity	Detection limit	Linear Range	References
BiBE	SWASV	Accumulation potential: −1.4 V Accumulation time: 180s	(0.112 ± 0.005) $\mu AL\mu g^{-1}$	0.054 μgL^{-1}	10–100 μgL^{-1}	[61]
PPh_3/MWCNTs/IL/CPE	SWASV	Accumulation potential: −1.2 V Accumulation time: 75s	0.585 μA/nM	2×10^{-2}nM	0.1–150 nM	[62]
Electropolymerization of arginine at MWCNT modified PGE	DPSV	Accumulation potential: −0.5 V Accumulation time: 5s	(0.463 ± 0.004) $\mu AL\mu g^{-1}$	2.12 μgL^{-1}	4.16–205.92 μgL^{-1}	[63]
Bi/Nafion/GC	DPV	Accumulation potential: −1.2 V Accumulation time: 180s	–	10 μgL^{-1}	5–1000 μgL^{-1}	[64]
$Mo_6S_3I_6$ NWs/GC	DPASV	Accumulation potential: −1.1 V Accumulation time: 240s	0.0893 $\mu AL\mu g^{-1}$	0.10 μgL^{-1}	0.5–150 μgL^{-1}	[65]
Bismuth Nanopowder Electrodes	SWASV	Accumulation potential: −1.35 V Accumulation time: 180s	3.28 ± 0.16 (mA/(ppb cm^2))	2.54 μgL^{-1}	–	[66]
L-MSNPs/CPE	ASSWV	Accumulation potential: −1.1 V Accumulation time: 60s	(0.579 ± 0.016) $\mu AL\mu g^{-1}$	0.3 μgL^{-1}	1.5–1000.0 μgL^{-1}	[67]
Bi-SPCNTEs	ASV	Accumulation potential: −1.4 V Accumulation time: 180s	0.5865 $\mu AL\mu g^{-1}$	0.8 μgL^{-1}	12–100 μgL^{-1}	[68]
MFEs	SWASV	Accumulation potential: −1.1 V Accumulation time: 120s	34.5 (10^7 μA $mol^{-1}L$)	9.70 (10^{-9}mol L^{-1})	9.8–1923 μgL^{-1}	[69]
BFE	SWASV	Accumulation potential: −1.4 V Accumulation time: 120s	–	1.39 μgL^{-1}	20–100 μgL^{-1}	[70]
3DAGN–STP/GCE further modified with a bismuth film	DPV	Accumulation potential: −1.1 V Accumulation time: 300s	9.05 (μA/(ppb cm^2)).	0.1 μgL^{-1}	1–70 μgL^{-1}	[71]
GO–MWCNTs/Bi hybrid nanocomposites	DPASV	Accumulation potential: −1.4 V Accumulation time: 180s	0.2358 $\mu AL\mu g^{-1}$	0.1 μgL^{-1}0.2 μgL^{-1}	0.5–30 μgL^{-1}	[72]
$MgSiO_3$/Nafion/GCE	SWASV	Accumulation potential: −1.4 V Accumulation time: 180s	Cd(II): 6.15 $\mu A\mu M^{-1}$	1.86×10^{-10} M	0.1–1.0 μM	[73]
SPEs	SWASV	Accumulation potential: −1.1 V Accumulation time: 120s	–	2.9 μgL^{-1}	10–3000 μgL^{-1}	[74]
Sb-CPE	SWASV	Accumulation potential: −1 V Accumulation time: 300s	–	1.4 μgL^{-1}	10–100 μgL^{-1}	[75]
SbFE	SWASV	Accumulation potential: −1 V Accumulation time: 60s	–	1.1 μgL^{-1}	25–80 μgL^{-1}	[20]
nsBiFE	SWASV	Accumulation potential: −1.2 V Accumulation time: 120s	–	0.4 μgL^{-1}	20–100 μgL^{-1}	[18]
SbFME	SWASV	Accumulation potential: −1.2 V Accumulation time: 120s	–	1.9 μgL^{-1}	20–100 μgL^{-1}	[21]
SWCNT-Cys	LSASV	Accumulation potential: OCP Accumulation time: 180s	(49 ± 2) x 10^{-3} $\mu AL\mu g^{-1}$	0·3 μgL^{-1}	1–300 μgL^{-1}	This work

BiBE: bismuth bulk electrode.
PPh_3/MWCNTs/IL/CPE: triphenylphosphine-modified carbon nanotube composite with a ionicliquid as pasting binder.
PGE: pencil graphite electrode.
Bi/Nafion/GC: GCE modified with Bi nanoparticles and Nafion.
$Mo_6S_3I_6$ NWs/GC: Molybdenum-chalcogenide-halide nanowires/glassy carbon electrode.
BTPP: N,N-bis(3(2-thenylidenimino)propyl)piperazine.
L-MSNPs:ligand modified silica nanoparticles.
L:N,N-bis(3(2-thenylidenimino)propyl)piperazine.
SPCEs: Screen-printed carbon electrodes.
SPEs: screen-printed electrodes.
MFEs: Mercury film electrodes.
SPCNTE: screen-printed carbon nanotubes electrodes.
BFE:bismuth film electrode.
3DAGNs: three-dimensional activated graphene networks.
STP: sulfonate-terminated polymer.
GO: Graphene oxide.
MWCNTs: multiwall carbon nanotubes.
$MgSiO_3$:nanostructured magnesium silicate hollow spheres.
Sb-CPE: carbon paste bulk-modified with antimony powder.
SbFE: antimony film electrode.
nsBiFE: nanostructured bismuth film electrode.
SbFME: antimony film microelectrode.

Table 3
Analytical application of GCE/SWCNT-Cys for the quantification of Cd(II) added to groundwater samples. Comparison to the results obtained with ICP-MS.

Samples	CD(II) added (μgL^{-1})	This sensor Cd(II) found	Recovery (%)	ICP-MS Cd(II) found
Groundwater	0.00	0.00	–	–
	10.0	10.1 ± 0.5	110.5	12 ± 1
	50.0	49 ± 4	106.7	51.7 ± 0.1
	100	100 ± 6	100.8	100 ± 2

ICP-MS: inductively coupled plasma-mass spectrometry.

Ir (IV) and Cu(II), indicating that there is no interference of these metals on the determination of Cd(II). The addition of 100 μgL^{-1} Tl(I) to the previous mixture produced a shifting in the Cd(II) oxidation peak potential of −20 mV as well as a decrease in the Cd(II) oxidation signal of 15%. Lower concentrations of Tl(I) did not produce any change. These results clearly demonstrate the excellent selectivity of GCE/SWCNT-Cys towards Cd(II) in the presence of other metals.

Table 2 summarizes the analytical parameters of different Cd(II) electrochemical sensors reported in the last years. Is important to remark that, at variance with most of the electrochemical sensors for Cd(II), where the preconcentration of Cd(II) is performed by reduction at very negative potentials [61–74,18,20,21], in the case of our sensor the preconcentration of Cd(II) is done at open circuit potential, through the specific Cd(II)–Cys complexation and subsequent medium exchange, largely decreasing the risk of possible interference of other metallic species able to be reduced at the preconcentration potential. The analytical performace of GCE/SWCNT-Cys is highly competitive since it presents similar or lower detection limits than most of the sensing strategies reported in the table and on of the widest linear range. Even when a strict comparison of sensitivities is not possible, the results obtained with our sensor are similar or better than those presented in Table 2. The difference in the affinity of Cys towards other metals [60] represent an additional contribution to the selectivity of the assay. Despite the time for the assay is longer than those reported for metal film electrodes, our sensor presents several advantages that make it a sensitive and selective alternativeto to quantify Cd(II).

To evaluate the practical application of the proposed electrochemical sensor, we determine the recovery of Cd (II) in groundwater samples taken from the city of Cordoba (Argentina) by triplicate using the GCE/SWCNT-Cys. The results are summarized in Table 3. Three different concentrations of Cd(II) were added to the groundwater samples (10.0, 50.0 and 100 μgL^{-1}) with excellent recoveries. The method was validated using ICP-MS with excellent agreement.

3.3. Conclusions

We reported here the advantages of a new electrochemical sensor for Cd(II) based on the modification of GCE with a dispersion of SWCNT covalently functionalized with Cys. At variance with most of the existing electrochemical sensing schemes, in this case we propose a preconcentration of Cd(II) at open circuit potential through the complex formation with Cys residues, minimizing the possibility of potential interference of other metallic cations. The combination of the electroactivity of SWCNT and the high affinity of Cys towards Cd(II) made possible the highly sensitive and selective quantification of Cd(II) even in the presence of an excess of several heavy metal ions. The proposed sensor was successfully used for the quantification of Cd(II) in groundwater samples with excellent correlation with ICP-MS, demonstrating to be a very interesting alternative for further applications in environmental monitoring.

Acknowledgements

The authors thank CONICET, SECyT-UNC, ANPCyT, MINCyT-Córdoba, Spanish Ministry of Economy and Competitiveness (MINECO) project ENE2013-48816-C5-5-R, and the Government of Aragon and the European Social Fund under project grant DGA-FSE-T66 CNN for the financial support.

Appendix A. Supplementary data

Supplementary data associated with this article can be found, in the online version, at http://dx.doi.org/10.1016/j.snb.2017.04.026.

References

[1] R. Wennrich, B. Daus, K. Müller, H. Stärk, L. Brüggemann, P. Morgenstern, Environ Poll. 165 (2012) 59–66.
[2] P. Ramnani, N.M. Saucedo, A. Mulchandani, Chemosphere 143 (2016) 85.
[3] M. Hesham, S. Sadeek, M. Abu Rehab, Z. Doa, Microchem. J 128 (2016) 1–6.
[4] C.R. Armendáriz, T. Garcia, A. Soler, Á.J. Gutiérrez Fernández, D. Glez-Weller, G. González, L.A. Hardisson de la Torre, C. Revert Gironés, Environ. Res. 143 (2015) 162–169.
[5] K.M.J.C. Dimpe, N. Ngila, P.N. Mabuba, Nomngongo, Phys. Chem. Earth 76–78 (2014) 42–48.
[6] B. Caballero-Segura, P. Ávila-Pérez, C.E. Barrera Díaz, J.J. Ramírez García, G. Zarazúa, R. Balan Ortiz-Oliveros, Intern. J. Environ Anal. Chem. 94 (2014) 1288–1301.
[7] Ö. Tunç Dede, Anal. Methods 8 (2016) 5087–5094.
[8] S. Su, M. He, N. Zhang, C. Cui, Anal. Methods 6 (2014) 1182–1188.
[9] O.F.M. Olorundare, T.A. Msagati, R.W.M. Krause, J.O. Okonkwo, B. Mamba, Int. J. Environ. Sci. Technol. 12 (2015) 2389–2400.
[10] C. Zhu, G. Yang, H. Li, Y. Lin, Anal. Chem 87 (2015) 230–249.
[11] A. Ghaemi, H. Tvakkoli, T. Mombeni, Mat. Sci. Eng. C 38 (2014) 186–191.
[12] V.K. Gupta, S. Kumar, R. Singh, L.P. Singh, S.K. Shvora, B. Sethi, J. Mol. Liquids 195 (2014) 65–68.
[13] E. Chow, D. Ebrahimi, J.J. Gooding, D.B. Hibbert, Analyst 131 (2006) 1051–1057.
[14] W. Yantasee, B. Charnhattakorn, G.E. Fryxell, Y. Lin, C. Timchalk, R. Shane Addleman, Anal. Chim. Acta 620 (2008) 55–63.
[15] J. Wang, J. Lu, S.B. Hocevar, P.A. Farías, B. Ogorevc, Anal. Chem. 72 (2000) 3218–3222.
[16] V. Jovanosvski, N.I. Hrastnik, S.B. Hocevar, Electrochem. Commun. 57 (2015) 1–4.
[17] G. Zhao, Y. Yin, H. Wang, G. Liu, Z. Wang, Electrochim. Acta 220 (2016) 267–275.
[18] T. Zidaric, V. Jovanovski, E. Menart, M. Zorko, M. Kolar, M. Veber, S.B. Hocevar, Sens. Actuators B. Chem. (2017) (in press).
[19] V. Rehaceka, I. Hotovya, M. Vojsa, T. Kupsb, L. Spiess, Electrochim. Acta 63 (2012) 192–196.
[20] V. Jovanosvki, S.B. Hocevar, B. Ogorevc, Electroanal 21 (2009) 2321–2324.
[21] M. Slavec, S.B. Hocevar, L. Baldrianova, E. Tesarova, J. Svancara, B. Ogorevc, K. Vytras, Electroanal 22 (2010) 1617–1622.
[22] N.B. Li, W.W. Zhu, J.H. Luo, H.Q. Luo, Analyst 137 (2012) 614–617.
[23] Z. Wang, H. Wang, Z. Zhang, X. Yang, G. Liu, Electrochim. Acta 120 (2014) 140–146.
[24] N. Yang, X. Chen, T. Ren, P. Zhang, D. Yang, Sens. Actuators B: Chem. 207 (2015) 690–715.
[25] S. Kumar, W. Ahlawat, R. Kumar, N. Dilbaghi, Biosens. Bioelectron. 70 (2015) 498–503.
[26] N. Wang, M. Lin, H. Dai, H. Ma, Biosens. Bioelectron. 79 (2016) 320–326.
[27] M. Hasanzadeh, N. Shadjou, M. De la Guardia, Trends Anal. Chem. 72 (2015) 123–140.
[28] Z. Wu, C. Xu, H. Chen, Y. Wu, H. Yu, Y. Ye, F. Gao, J. Phys. Chem. Solids 74 (2013) 1032–1038.
[29] H. Bagheri, A. Afkhami, H. Khoshsafar, M. Rezaei, S.J. Sabounchei, S. Mehdi, Anal. Chim. Acta 870 (2015) 56–66.
[30] N. Ruecha, N. Rodthongkum, D.M. Cate, J. Volckens, O. Chailapakul, C.S. Henry, Anal. Chim. Acta 874 (2015) 40–48.
[31] Y. Zhang, M. Qi, G. Liu, Electroanal 27 (2015) 1–10.
[32] A. Afkhami, H. Bagheri, H. Khoshsafar, M. Saber-Tehrani, M. Tabatabae, A. Shirzadmehr, Anal.Chim. Acta 746 (2012) 98–106.
[33] G.D. Vukoviíc, A.D. Marinkovic, M. Coliíc, M. Ristic, R. Aleksiíc, A.A. Periíc-Grujiíc, P.S. Uskokoviíc, Chem. Eng. J. 157 (2010) 238–248.
[34] P. Blondeau, F.X. Rius-Ruiz, A. Düzgün, J. Riu, F.X. Rius, Mater. Sci. Eng. C 31 (2011) 1363–1368.
[35] G.D. Vukoviíca, A.D. Marinkoviíc, S.D. Skapinc, M. Ristic, R. Aleksic, A.A. Peric-Grujic, P.S. Uskokovic, Chem. Eng. J. 173 (2011) 855–865.
[36] G. Berthon, Pure Appl. Chem. 67 (1995) 1117–1240.
[37] N.M. Bandaru, N. Reta, H. Dalal, A.V. Ellis, J. Shapter, N.H. Voelcker, J. Hazard. Mater. 261 (2013) 534–541.
[38] H.A.M. Elmahadi, G.M. Greenway, J Anal. Atom. Spectrom. 8 (1993) 1009–1014.
[39] P. Dalmasso, M.L. Pedano, G.A. Rivas, Electroanal 27 (2015) 2164–2170.
[40] E.N. Primo, F.A. Gutierrez, G.L. Luque, P.R. Dalmasso, A. Gasnier, Y. Jalit, M. Moreno, M.V. Bracamonte, M. Eguílaz Rubio, M.L. Pedano, C. Rodríguez, N.F. Ferreyra, M.D. Rubianes, S. Bollo, G.A. Rivas, Anal. Chim. Acta 805 (2013) 19–35.
[41] Y. Wei, X. Ling, L. Zou, D. Lai, H. Lu, Y. Xu, Colloid Surf. A 482 (2015) 507–513.
[42] M. Eguílaz, F. Gutierrez, J.M. González-Domínguez, M.T. Martínez, G. Rivas, Biosens. Bioelectron. 86 (2016) 308–314.
[43] J. Morton, N. Havens, A. Mugweru, A.K. Wanekaya, Electroanal 21 (2009) 1597–1603.

[44] Y. Mori, M. Seki, Org. Synth. 11 (2007) 28.
[45] I. Photaki, T. Papadimitriou, C. Sakarellos, P. Mazarakis, L. Zervas, J. Am. Chem. Soc. 92 (1970) 2683–2687.
[46] D.A. Pearson, M. Blanchette, M.L. Baker, C.A. Guindon, Tetrahedron Lett. 30 (1989) 2739–2742.
[47] R.A. Meyers, Interpretation of infrared spectra, a practical approach, in: John Coates (Ed.), Encyclopedia of Analytical Chemistry, John Wiley & Sons Ltd, Chichester, 2000.
[48] C.N.R. Rao, Chemical Applications of Infrared Spectroscopy, Academic Press, New York and London, 1963.
[49] M. Amiri, H. Eynaki, Y. Mansoori, Electrochim. Acta 123 (2014) 362–368.
[50] S.F. Parker, Chem. Phys. 424 (2013) 75–79.
[51] M.S. Dresselhaus, G. Dreseelhaus, M. Hofmann, Vib. Spectrosc. 45 (2007) 71–81.
[52] S. Niyogi, E. Bekyarova, M.E. Itkis, H. Zhang, K. Shepperd, J. Hicks, M. Sprinkle, C. Berger, C.N. Lau, W.A. de Heer, E.H. Conrad, R.C. Haddon, Nano Lett. 10 (2010) 4061.
[53] S. Stankovich, D. Dikin, R.D. Piner, K. Kohlhaas, A. Kleinhammes, Y. Jia, Carbon 45 (2007) 1558–1565.
[54] M.V. Bracamonte, G.I. Lacconi, S.E. Urreta, L.E.F. Foa Torres, J. Phys. Chem. C 118 (2014) 15455–15459.
[55] P. Canete-Rosales, V. Ortega, A. Alvarez-Lueje, S. Bollo, M. Gonzalez, A. Ansón, M.T. Martinez, Electrochim. Acta 62 (2012) 163.
[56] A. Ansón-Casaos, M. Gonzalez, J.M. Gonzalez-Dominguez, M.T. Martinez, Langmuir 27 (2011) 7192–7198.
[57] https://srdata.nist.gov/xps/query_chem_name_detail.aspx?ID_NO=2410&CName=DL-cysteine
[58] K. Yang, M.Y. Gu, Y.P. Guo, X.F. Pan, G.H. Mu, Carbon 47 (2009) 1723–1737.
[59] J.M. González-Domínguez, F.A. Gutiérrez, J. Hernández, A. Ansón-Casaos, M.D. Rubianes, G. Rivas, M.T. Martínez, J. Mater. Chem. B 3 (2015) 3870–3884.
[60] H. Sigel, C.P. Da Costa, R.B. Martin, Coord. Chem. Rev. 219–221 (2001) 435–461.
[61] K.C. Armstrong, C.E. Royce, N. Dansby-Sparks, J.Q. Chambers, Z.-L. Xue, Talanta 82 (2010) 675–680.
[62] H. Bagheri, A. Afkhami, H. Khoshsafar, M. Rezaei, A. Shirzadmehr, Sens. Actuators B: Chem. 186 (2013) 451–460.
[63] E. Roy, S. Patra, R. Madhuri, P.K. Sharma, RSC Adv. 4 (2014) 56690–56700.
[64] H. Yang, J. Li, X. Lu, G. Xi, Y. Yan, Mater. Res. Bull. 48 (2013) 4718–4722.
[65] H. Lin, M. Li, D. Mihailovi, Electrochim. Acta 154 (2015) 184–189.
[66] G.-J. Lee, C.K. Kim, M.K. Lee, C.K. Rhee, Electroanal 22 (2010) 530–535.
[67] A. Afkhami, F. Soltani-Felehgari, T. Madrakian, H. Ghaedi, M. Rezaeivala, Anal. Chim. Acta 771 (2013) 21–30.
[68] U. Injang, P. Noyrod, W. Siangproh, W. Dungchai, S. Motomizu, O. Chailapakul, Anal. Chim. Acta 668 (2010) 54–60.
[69] M. Firmino de Oliveira, A.A. Saczk, L.L. Okumura, A. Pires Fernandes, M. de Moraes, N. Ramos Stradiotto, Anal. Biol. Anal. Chem. 380 (2004) 135–140.
[70] J. Li, J. Zhang, H. Wei, E. Wang, Analyst 134 (2009) 273–277.
[71] X. Yuan, Y. Zhang, L. Yang, W. Deng, Y. Tan, M.M. Qingji Xie, Analyst 140 (2015) 1647–1654.
[72] H. Huang, T. Chen, X. Liu, H.m Ma, Anal. Chim. Acta 852 (2014) 45–54.
[73] R.-X. Xua, X.-Y. Yu, C. Gao, Y.-J. Jiang, D.-D. Han, J.-H. Liu, X.-J. Huang, Anal. Chim. Acta 790 (2013) 31–38.
[74] R. Güell, G. Aragay, C. Fontàs, E. Anticó, A. Merkoçi, Anal. Chim. Acta 627 (2008) 219–224.
[75] E. Svobodova-Tesarova, L. Baldrianova, M. Stoces, I. Svancara, K. Vytras, S.B. Hocevar, B. Ogorevc, Electrochim. Acta 56 (2011) 6673–6677.

Biographies

Fabiana A. Gutierrez obtained her Ph. D. in Chemistry (2009) from Cordoba National University (Argentina). The Ph.D studies were performed in the group of Electrochemistry and Surface and where based on the functionalization of metal surfaces. She did the postdoctoral training on electrochemical biosensors based on the functionalization of carbon nanotubes and magnetic nanoparticles in the group of Biosensors at the Physical Chemistry Department, Faculty of Chemical Sciences (Cordoba National University). At present, Dr. Gutierrez is an active member of the Biosensor§ Group and her research interests are focused on electrochemical and plasmonics genosensors and immunosensors: design, characterization and analytical applications for the quantification of clinical and environmental biomarkers.

Jose Miguel González-Domínguez is a postdoctoral researcher at the University of Castilla-La Mancha. He obtained his B.S. in Chemistry in 2007 (University of Extremadura, Spain) and his PhD degree in Organic Chemistry in 2012 from the University of Zaragoza (Spain), while working at the Institute of Carbon Chemistry-CSIC. He held there a postdoctoral position in 2012-2013. He was then a postdoctoral researcher in 2013-2015 at the University of Trieste (Italy), Department of Chemical Sciences, being the first year as a Marie Curie fellow. In 2015 he joined the Organic Chemistry area of the University of Castilla-La Mancha (Spain) as a 'Juan de la Cierva' fellow. Along his scientific track he has been awarded with several young researchers awards, including the Extraordinary Doctorate award (University of Zaragoza), the Spanish Royal Society of Chemistry prize (specialized polymer group) and was finalist to the Spanish Carbon Group's young researchers award. His main focuses are carbon nanostructures, their chemical functionalization, and their polymer composites for structural, sensing and biomedical applications.

Alejandro Ansón Casaos was born in Zaragoza in 1978. He obtained his PhD in Physical Chemistry from the University of Zaragoza in June 2005 and is a Research Scientist at Instituto de Carboquimica ICB-CSIC since August 2012. His current research includes fundamentals and applications of carbon nanomaterials, mainly carbon nanotubes and graphene oxide, and their colloids. Most specifically, he is interested in the study of physicochemical properties that are relevant for applications in photocatalysis, photovoltaics, energy storage, sensors, and polymer composites.

Javier Hernández-Ferrer received his diploma in Chemistry in 2001 and PhD in Materials Science in 2008 at the University of Alicante. Currently, he is part of the Group of Carbon Nanostructures and Nanotechnology, at the Institute of Carbochemistry in Zaragoza (Spain). His resarch activities are focused on the electrochemical properties and applications of carbon nanomaterials and hybrid materials.

María D. Rubianes obtained her Ph. D. in Chemistry (2005) from the Cordoba National University (Argentina). She did the postdoctoral training in the group of Polymers at the Organic Chemistry Department, Faculty of Chemical Sciences (Cordoba National University). At present, she is Adjunt Professor at the Department of Physical Chemistry, Faculty of Chemical Sciences and Independent Researcher at Argentine Research Council (CONICET). Dr. Rubianes is an active member of the Biosensors Group at the Physical Chemistry Department, and her research interests are focused on the synthesis and characterization of modified polymers for the functionalization of nanostructured materials.

María Teresa Martinez graduated in Chemistry (1976) and Chemical Engineering (1978) and received her PhD degree in the field of Chemistry from Zaragoza University in 1982. Currently she is Research Professor at the Institute of Carbon-Chemistry (CSIC) where she previously worked as CSIC Research Fellow and Senior Research Scientist. She was director of the Institute of Carbon-Chemistry between 2002 and 2006 and from 1995 to 2014 she led the group of Carbon Nanotubes and Nanotecnology. She worked as visiting Professor in International Research Institutions of Germany, United Kingdom, USA and Chile. She was a member of the European Coal and Steel Experts Committee for "Coal Conversion Area" (2000-2002) and co-chairman of the "Strategic Research Area" of the Hydrogen Platform for the VI Framework Programme 2004. At National level she has been member of the Research and Development Advisory Committee of the Regional Government (2004-2014) and member of the CSIC Chemical Science and Technologies Area (2001-2006). Prof. Martinez has developed her research career in a multidisciplinary sphere in the field of material science, energy and environment and for the last 20 years she has approached these fields from the Nanotechnology developing nanomaterials for Energy, Enviromental and Biotechnological applications. Prof. Martinez research is focused on Nanoscience and Nanotechnology, her expertise is the development of materials (synthesis, functionalization and processing of hybrid and compounds materials) based on carbon nanostructures; carbon nanotubes, graphene and graphene quantum dots. Today Prof. Martinez and her group (Carbon Nanostructures and Nanotechnology founded in 1995) develop innovative and high quality research at the forefront of science combining physics, chemistry and engineering approaches fostering interdisciplinary research. She is so far, the co-author of over than 200 peer-reviewed publications and hundreds of communications to International Congress in these fields.

Gustavo A. Rivas obtained his Ph. D. in Chemistry from Cordoba National University (Cordoba, Argentina). He did the postdoctoral training at University of Valence, Valence (Spain) and at New Mexico State University, Las Cruces (USA). At present, he is full professor at Cordoba National University and Superior Researcher at Argentine Research Council (CONICET). Dr. Rivas was the head of the Department of Physical Chemistry at the Faculty of Chemical Sciences (2008–2010). He was President of the Argentinean Society of Analytical Chemists between 2005 and 2007. From 2016 Professor Rivas is Academic of the National Academy of Sciences of Argentina. He is the recipient of the Ranwell Caputto Award from National Academy of Sciences of Argentina (2001), Rafael Labriola Award from Argentinean Society of Chemistry (2004), and Konex Award in Nanotechnology (2013). He has over 150 publications including peer-reviewed papers and book chapters, with more than 7500 citations and impact factor of 47. His research interests focus on the design and characterization of electrochemical (bio)sensors based on nanostructured materials for the quantification of (bio)markers of clinical and environmental relevance.